Supplementary Information

Self-supporting and bifunctional Cu-based electrocatalysts with porous structures as superior working electrode for alkaline water splitting

Xiaomei Xu[a], Kefang Yang[a], Jiazi She[a], Yanshui Zhai[a], Meihua Zhou[a], Ruihong Deng[a], Zhimei Li[a, *], Hu Cai[a, *].

[a]School of Chemistry and Chemical Engineering, Nanchang University, 999 Xuefu Avenue, Nanchang 330031, China.

*** Corresponding author**

E-mail: lizhimei@ncu.edu.cn (Zhimei Li)

E-mail: caihu@ncu.edu.cn (Hu Cai)

Materials: Sodium hydroxide, Potassium hydroxide, Anhydrous ethanol, Sodium chloride, Sodium sulfate, phenolphthalein, Methyl red were provided by Xilong Scientific Co., Ltd. Carbon disulfide were purchased by Shanghai Maclean Biochemical Technology Co., ltd.

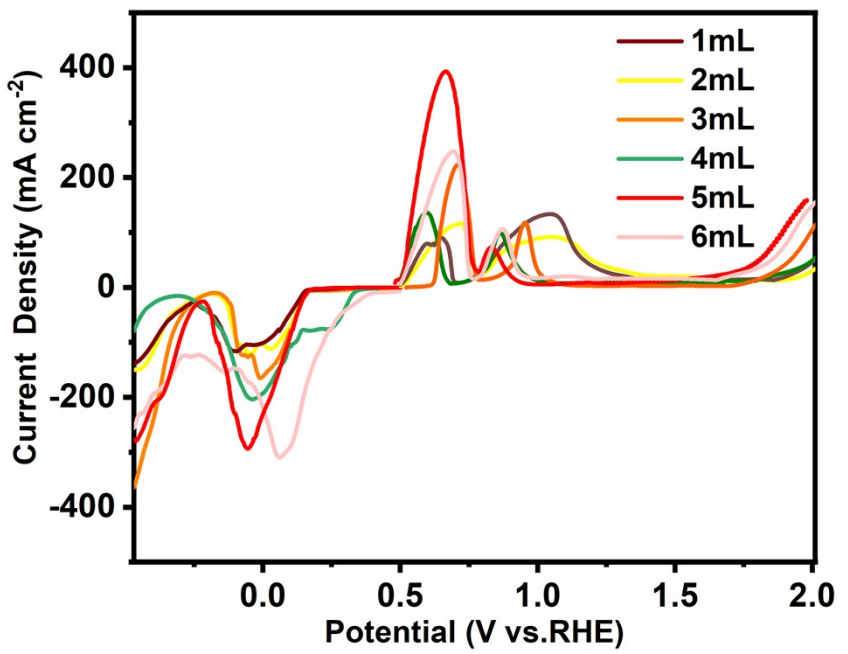

Fig.S1. Comparison of catalytic activities with different amount of CS_2.

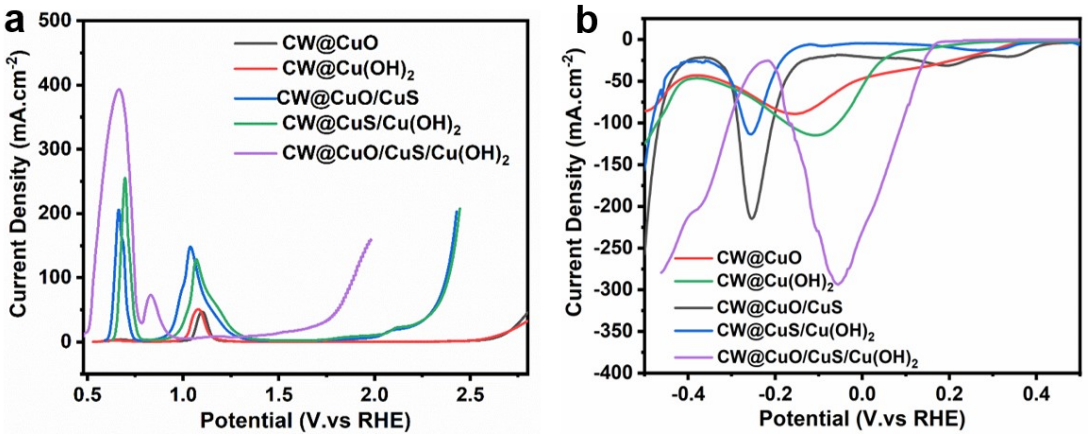

Fig. S2. (a, b) LSV of different samples.

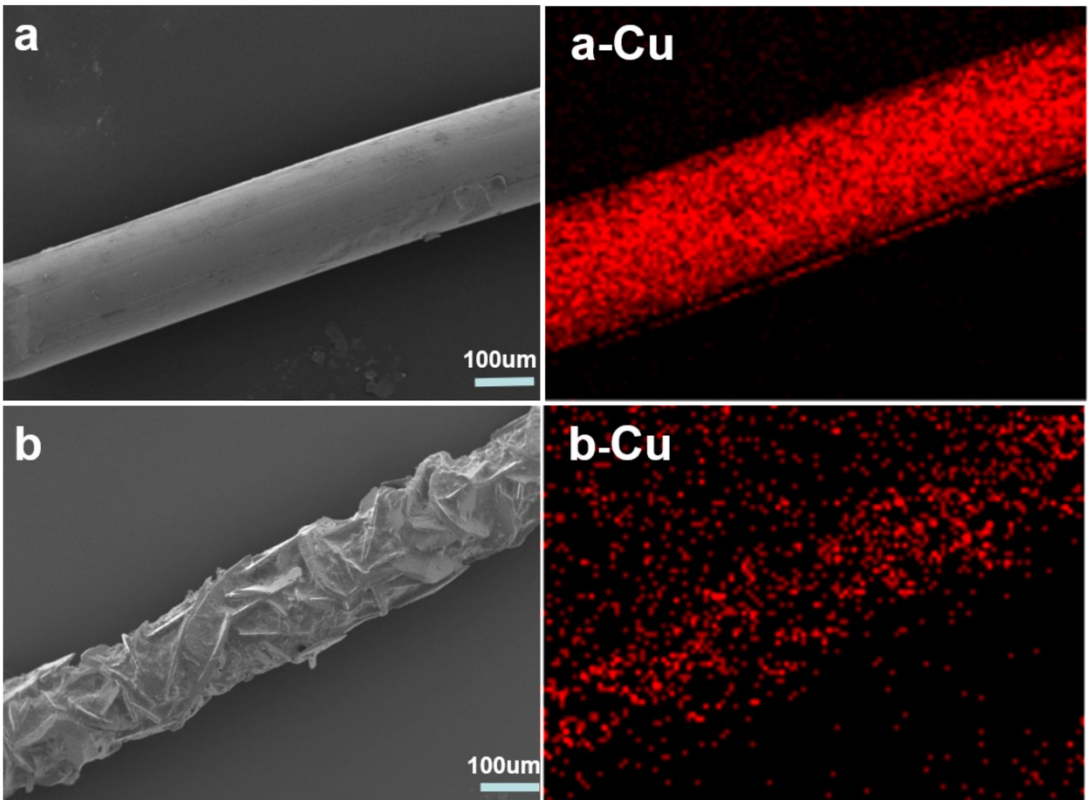

Fig. S3. The surface morphology SEM images and elements distributions of the original CWs(a) and etched CWs (b).

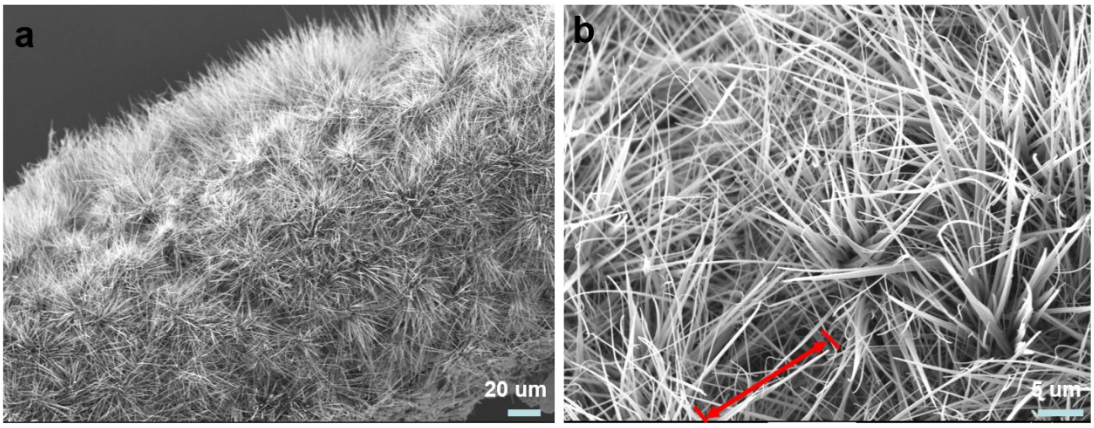

Fig. S4. Morphology characterization of CW@$Cu^{I/II}O$/Cu $(OH)_2$ Nps electrode (a) and (b).

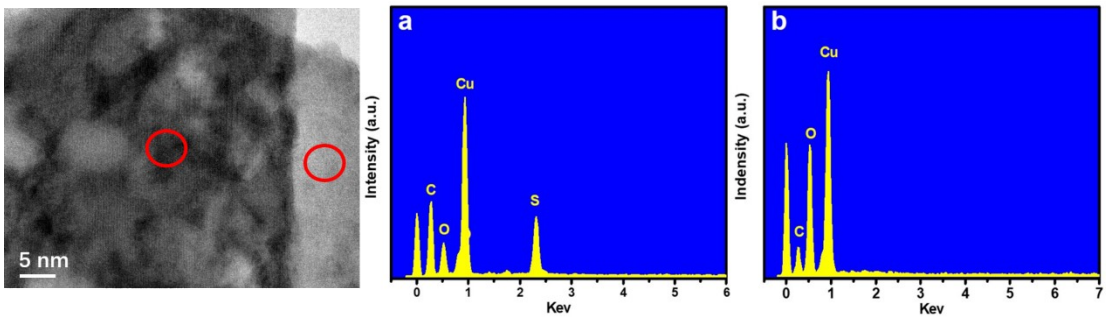

Fig. S5. TEM images of CW@$Cu^{II}O/Cu^{II}S$/Cu $(OH)_2$ Nps electrode and EDS spectra of $Cu^{II}S$ (a) and $Cu^{II}O$/Cu $(OH)_2$ Nps (b).

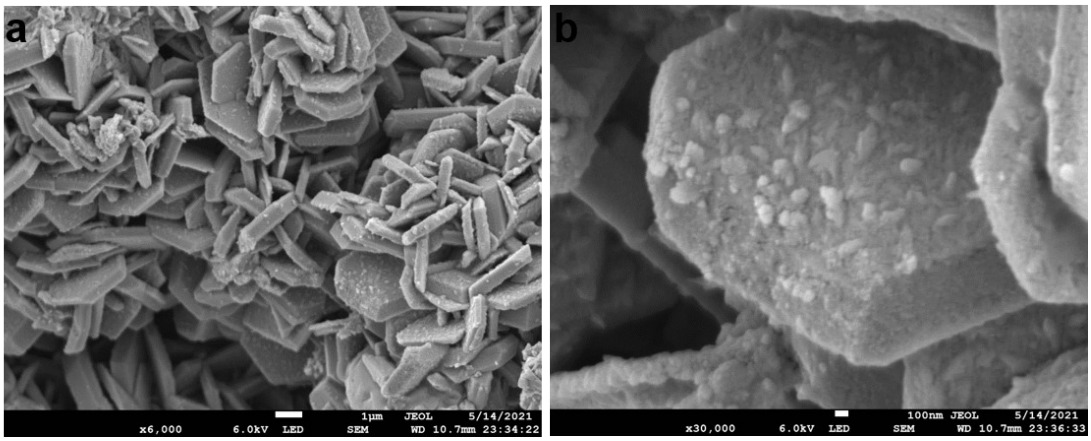

Fig. S6. (a, b) The surface morphology of the working electrode after oxidation and reduction reaction at different magnification.

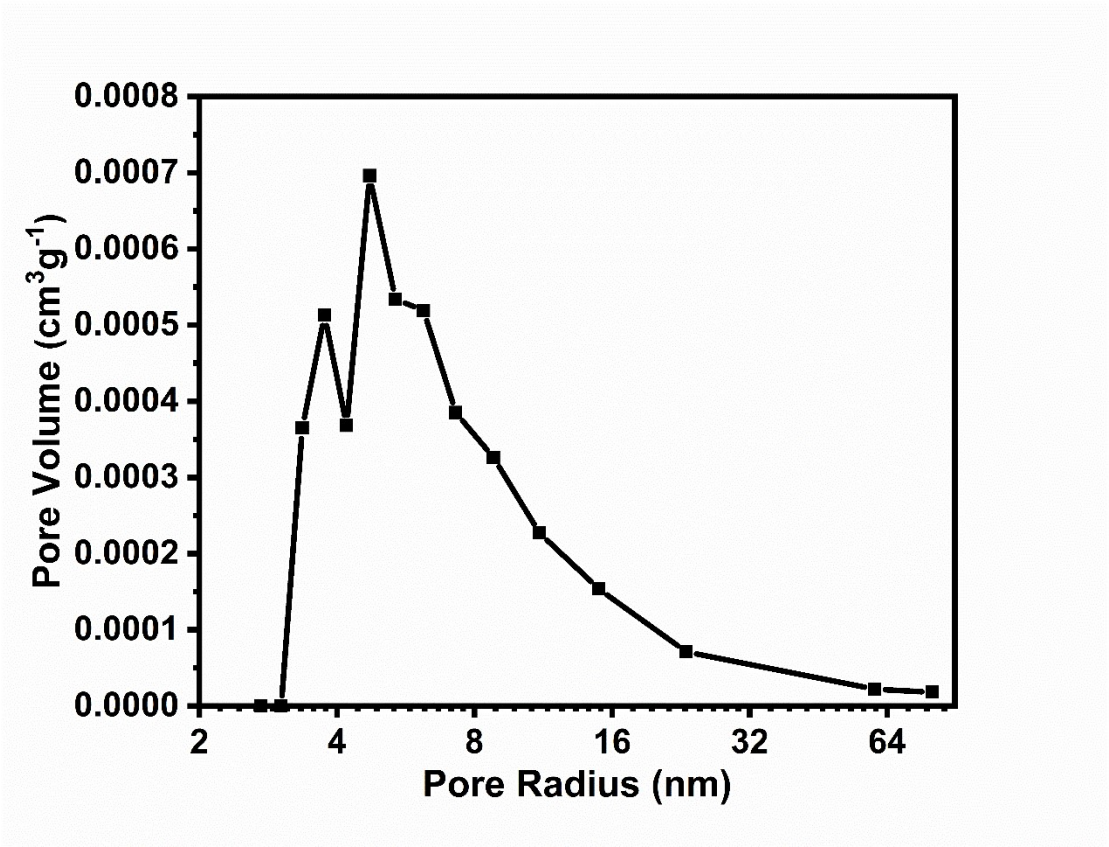

Fig. S7. Pore size distribution for CW@ $Cu^{I/II}O$ /Cu $(OH)_2$ NPs sample.

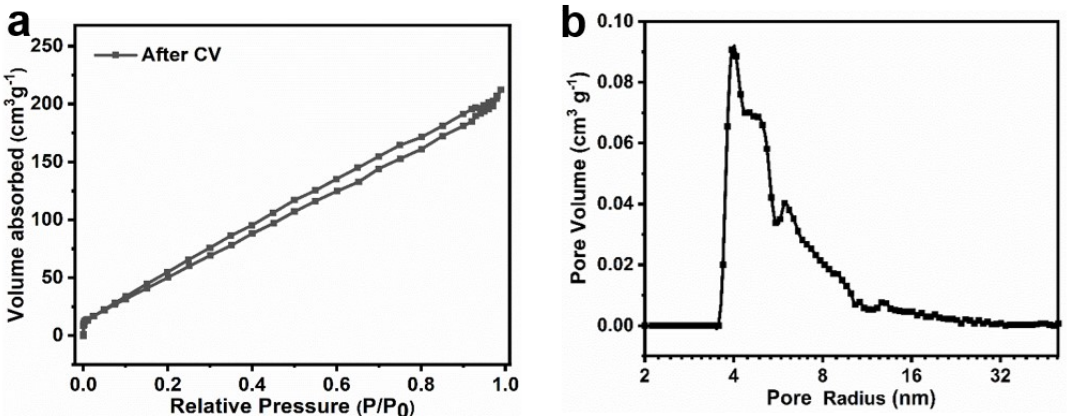

Fig. S8 (a) N_2 adsorption-desorption analysis results after oxidation and reduction experiment of the $Cu^{II}O/Cu^{II}S/Cu(OH)_2$ Nps; (b) Pore size distribution for samples after oxidation and reduction experiment.

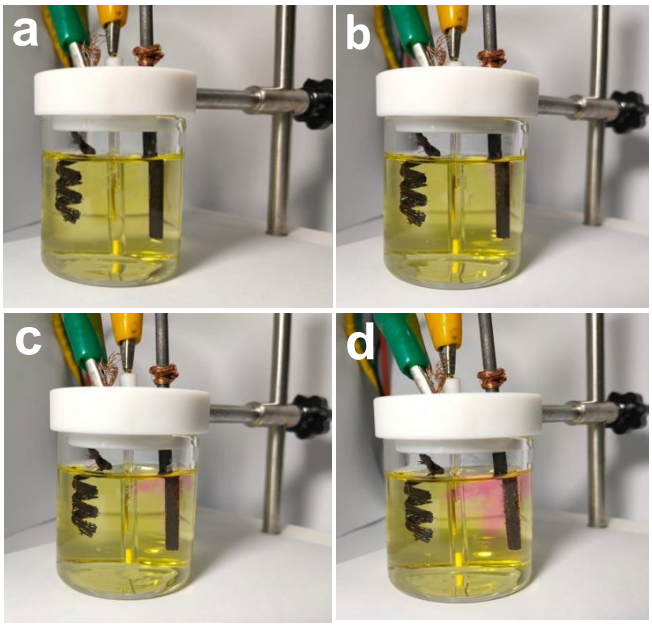

Fig. S9. The result of the color-change-process around the carbon rod when methyl orange is added at +0.06 V in 1M sodium sulfate solution.

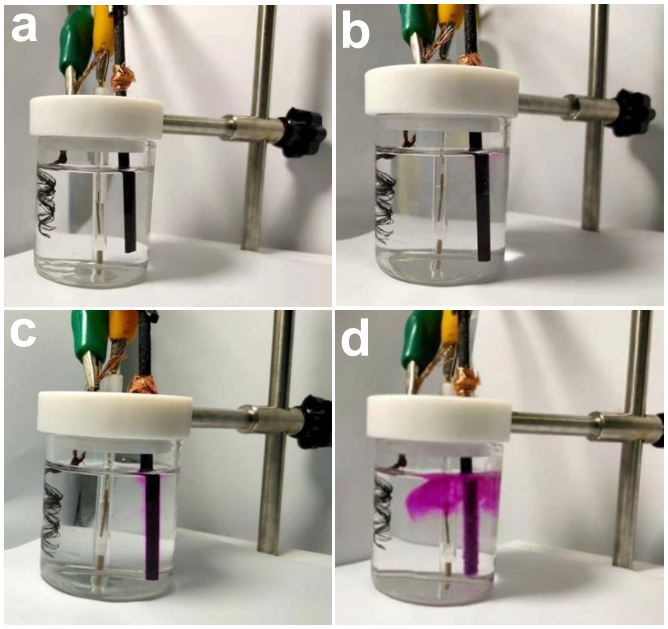

Fig. S10. The result of the color-change-process around the carbon rod when methyl orange is added at -0.06V in 1M sodium sulfate solution.

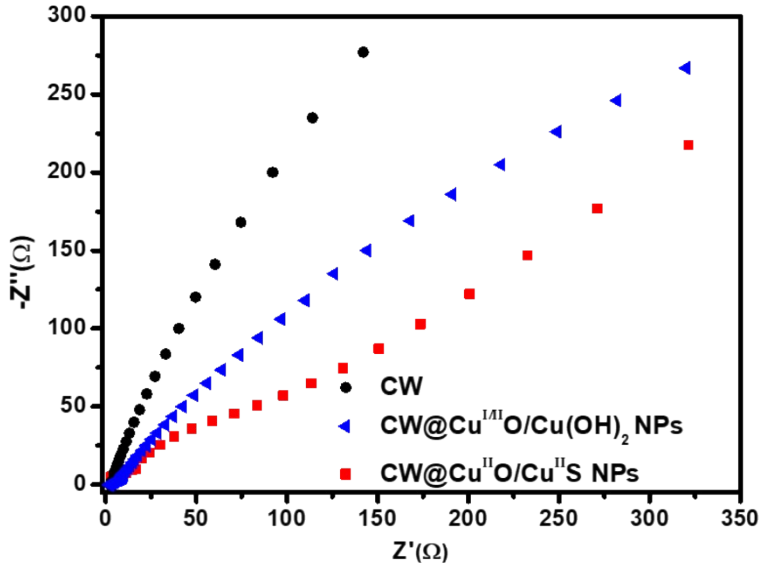

Fig. S11. Nyquist plots of samples indicated in 1M KOH.

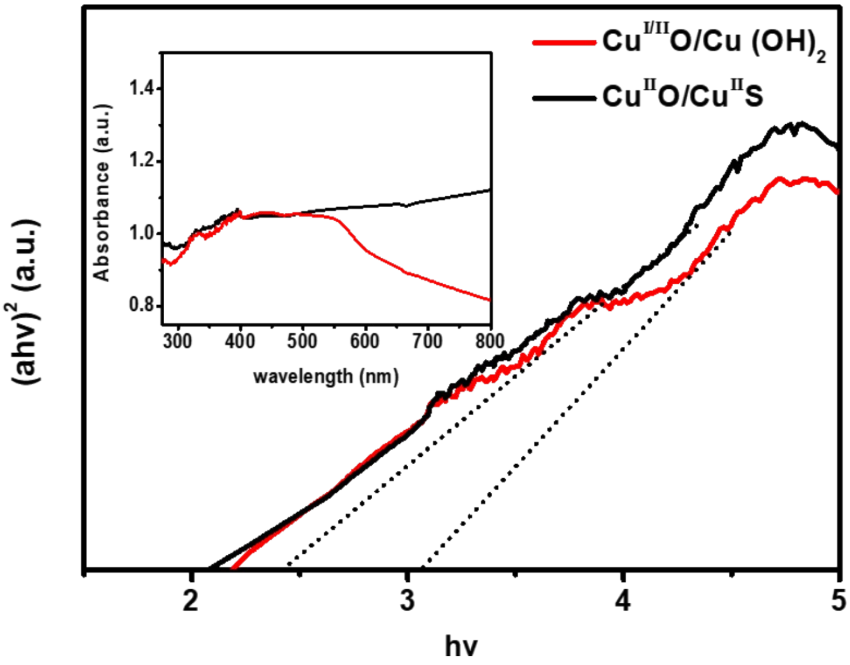

Fig. S12. Tauc plot of @Cu^{II}O/Cu^{II}S/Cu (OH)$_2$ and Cu$^{I/II}$O/Cu (OH)$_2$ samples. The inset is UV-Vis diffuse reflectance spectra (DRS).

Table S1. Electrocatalytic performance data of different samples.

sample	CW@CuO	CW@$Cu(OH)_2$	CW@CuO/CuS	CW@CuS/$Cu(OH)_2$	CW@CuO/CuS/$Cu(OH)_2$
Potential (V vs. RHE) for OER	**2.64**	**2.64**	**1.94**	**1.94**	**1.39**
η_{10} (mV)	**410**	**410**	**610**	**610**	**160**
Potential(V vs. RHE) for HER	**>-0.5**	**-0.47**	**-0.46**	**-0.48**	**-0.267**
η_{100} (mV)	**>500**	**470**	**460**	**480**	**267**

Table S2. Element content results for samples.

Samples	S	Cu	O
CW @ $Cu^{II}O/Cu^{II}S/Cu(OH)_2$ NPs	22.57	60.26	17.17
CW @$Cu^{I/II}O/Cu(OH)_2$ NPs	0.00	59.17	40.83

Table S3. BET surface area of samples.

Samples	Specific Surface Area (m^2/g)
CW@ $Cu^{II}O/Cu^{II}S/Cu(OH)_2$ Nps	5.56
CW @$Cu^{I/II}O/Cu(OH)_2$ Nps	27.73

Table S4. Mechanism speculation.

Potential (V vs. RHE)	Gas	Transformation	Half Reaction (1 M KOH)
< -0.27 V	O_2	/	(+) $4OH^- == 2H_2O+O_2\uparrow+ 4e^-$
	H_2	/	(-) $2H_2O + 2 e^- = 2OH^- +H_2\uparrow$
		Total reaction equation	$2H_2O = 2 H_2\uparrow+ O_2\uparrow$
0.48 V ~ -0.27 V	O_2	$Cu^{II}S \rightarrow Cu^{I}S$ $Cu^{II}O/ Cu(OH)_2 \rightarrow Cu^{I}O$	(-) $CuS + H_2O +2CuO+ Cu(OH)_2$ $+4 e^- = Cu_2S +Cu_2O+4OH^-$
		/	(+) $4OH^- == 2H_2O+O_2\uparrow+ 4 e^-$
		Total reaction equation	$CuS +2CuO+ Cu(OH)_2= Cu_2S$ $+Cu_2O+ O_2\uparrow +H_2O$
0.51 V ~0.93V	H_2	$Cu^{I}S \rightarrow Cu^{II}S$ $Cu^{I}O \rightarrow Cu^{II}O$ $/Cu(OH)_2$	(+) $Cu_2S+Cu_2O+4OH^- =$ $CuS+2CuO+Cu(OH)_2 +H_2O +4e^-$
		/	(-) $4H_2O + 4 e^- = 4OH^-+2H_2\uparrow$
		Total reaction equation	$Cu_2S+Cu_2O+3H_2O=CuS+ 2CuO$ $+ Cu(OH)_2+2H_2\uparrow$
>1.48V	O_2	/	(+) $4OH^- == 2H_2O+O_2\uparrow+ 4 e^-$
	H_2	/	(-) $2H_2O + 2 e^- = 2OH^-+H_2\uparrow$
		Total reaction equation	$2H_2O = 2 H_2\uparrow+ O_2\uparrow$

Table S5. Gas chromatogram of air in the environment (O: N=1:3).

	time	peak area	gas
1	**0.71**	**573.3**	**O_2**
2	**0.752**	**1862.2**	**N_2**

Table S6. Gas chromatogram of oxygen.

	time	peak area	gas
1	**0.722**	3796.9	**O_2**
2	**0.77**	86.2	**N_2**

Table S7. Gas chromatogram of hydrogen.

	time	peak area	gas
1	**0.69**	3587.5	**H_2**
2	**0.73**	119.1	**O_2**
3	**0.78**	301.4	**N_2**

Table S8. Comparison of HER and OER activities with different sulfur-copper compounds in 1M KOH

Electrocatalyst	Current Density ($mA.cm^{-2}$)	η for OER (mV)	Tafel slop ($mV.dec^{-1}$)	Current Density ($mA.cm^{-2}$)	η for HER (mV)	Tafel slop ($mV.dec^{-1}$)	Ref.
Cu_2S NRs @CoS	50	275	54	50	235	121	*Electrochimica Acta.*, 2019, **296**, 1035.
CoO@Cu_2S	10	277	62	/	/	/	*Appl. Surf. Sci.*, 2021, **555**, 149441.
CuS/SnS_2/rGO	100	264	47	/	/	/	*Dalton Trans.*, 2021, **50**, 5530-5539
Co_3S_4/CuS @CoNi-LDH	10	220	90.78	*10*	*136*	136.3	*Mater Res Lett.,* 2022,**10**, 2095235.
Ni-CuS	10	390	96.8				*Catal. Sci. Technol.*, 2019, **9**, 406-417.
Co_9S_8/Cu_2S	10	195	143.5	*10*	*165*	80.2	*ACS Appl. Mater. Interfaces.,* 2021, **13**, 9865–9874.
Co9S8/Cu_2S	10	220	372	*90.78*	*136*	126.3	*J. Energ. Chem.*, 2019, **39**, 61-67.
CoS2/CuS	10	/	/	*10*	*85*	52	*ACS Sustainable Chem. Eng.* 2019, **7**, 14016–14022.
CuS–Ni3S2	100	*377*	*142*	/	/	/	*Inorg. Chem. Front.,* 2019, **6**, 293-302.
This work	**10**	**160**	**34**	**100**	**230**	**119**	**Our work**